MINT: A multivariate integrative method to identify reproducible molecular signatures across independent experiments and platforms

F. Rohart [1], A. Eslami [2], N. Matigian [1], S. Bougeard [3], K-A. Lê Cao [1,*]

[1]The University of Queensland Diamantina Institute,
Translational Research Institute, QLD 4102, Australia,

[2] Department of Psychiatry, Faculty of Medicine, University of British Columbia,
Vancouver, BC Canada V6T 2A1

[3] Department of Epidemiology,
French agency for food, environmental and occupational health safety (ANSES),
22440 Ploufragan, France

Abstract

The solution to identify a reliable molecular signature in transcriptomics high-throughput experiments is to increase sample size by combining independent but related studies. However, those data sets are generated using different protocols and technological platforms, which results in unwanted systematic variation that strongly confounds the integrative analysis results. We introduce a Multivariate INTegrative method, MINT, that identifies a highly reproducible, accurate and predictive gene signature to classify sample phenotypes while accounting for platform and study variation. MINT led to superior and unbiased classification performance compared to other existing methods, and identified highly relevant gene signatures when integrating two multi-transcriptomics studies.

1 Introduction

With the advent of high-throughput technologies, many studies using microarray and RNA-sequencing technologies have reported finding biomarkers or gene signatures that can distinguish disease subgroups, predict cell phenotypes or classify responses to drugs. However, few of these findings are reproduced when assessed in subsequent studies and even fewer lead to clinical applications (Pihur *et al.*, 2008; Kim *et al.*, 2016). This is most likely a consequence of analysing high-dimensional data with a small sample size (< 20) per experiment compared to several thousands of variables (genes, transcripts). Combining raw data from independent experiments in an integrative analysis is one solution to increase sample size, which would in turn improves both statistical power and reproducibility across studies (Lazar *et al.*, 2012).

Integrating transcriptomic studies with the aim of classifying biological samples based on an outcome of interest (integrative classification), remains difficult in practice because of technical differences among studies, such as different experimental protocols or the use of different technological platforms. In combination, these technical factors contribute to the so-called 'batch-effects', which refer to cross-study, cross-platform or unwanted systematic variation (Gagnon-Bartsch and Speed, 2012). The MicroArray Quality Control (MAQC) project demonstrated that technological platform is an important confounder that can hinder the production of reproducible research in transcriptomic studies (Shi *et al.*, 2006). That study reported poor overlap of differentially expressed genes using different microarray platforms ($\sim 60\%$) and later highlighted low concordance between microarray and RNA-seq technologies (Su *et al.*, 2014). Therefore, confounding effects and systematic variation must be accounted for when combining independent studies in order to reliably identify genuine biological variation within and between studies. Several batch-effect removal methods have been proposed to normalise and combine microarray datasets such as ComBat (Johnson *et al.*, 2007), Batch Mean-Centering (Sims *et al.*, 2008), LMM-EH-PS (Listgarten *et al.*, 2010), RUV-2 (Gagnon-Bartsch and Speed, 2012) and YuGene (Lê Cao *et al.*, 2014). ComBat, in particular, has been successfully applied by the scientific community (over 1,000 citations).

Commonly, batch-effect removal methods are only the first step of a transcriptomic analysis. The second step fits a statistical model to classify biological samples and predict the class membership of new samples. A range of classification methods exists for these purposes, including machine learning approaches (e.g. random forests, Breiman 2001 or Support Vector Machine) as well as multivariate linear approaches (Linear Discriminant Analysis LDA, Partial Least Square Discriminant Analysis PLSDA, Barker and Rayens 2003). In addition, both classification and prediction accuracy can be improved by reliably identifying key discriminant or predictive biomarkers (genes or transcripts) among the thousands that are measured. This also enables better characterisation of the studied biological system. Biomarker selection is often performed using two-step procedures by combining univariate tests (e.g. t-, ANOVA) to select biomarkers prior to their inclusion in classification models, or by applying methods with built-in biomarker selection, such as machine learning methods (Kuhn 2008) or sparse multivariate models (Lê Cao *et al.*, 2011) that include ℓ^1 penalties (Tibshirani, 1996).

In the context of integrative classification, the standard approach is to sequentially accommodate for batch effects before selecting discriminant biomarkers and then (or simultaneously) classifying biological samples. Recent developments with multivariate methods include sparse PLS-DA (sPLS-DA, Lê Cao *et al.* 2011) that performs classification and variable selection in a single step, and our mgPLS that corrects for unwanted variation across independent studies in a classification framework, but does not perform variable selection (Eslami *et al.*, 2013, 2014). Although the sequential approach enables integrative classification, it has inherent shortcomings that have been so far largely ignored in the literature. The major pitfall of the sequential approach is a risk of over-optimistic results due to a statistical modelling that overfits the training set and can not be reproduce on test sets. Moreover, we observed that most proposed classification models were not objectively validated on an external and independent test set, which can result in spurious conclusions and limit the benefit of translating the result to a clinical tool (Kim *et al.*, 2016). For instance, most classification methods require the choice of a parameter (e.g. sparsity), which is usually optimised with cross-validation (data are divided into k subsets or 'folds' and each fold is used once as an internal test set). Unless the removal of batch-effects is performed independently on each fold, the folds are not independent and this leads to over-optimistic classification accuracy on the internal test sets. Hence, batch removal methods must be used with caution. For instance, ComBat can not remove unwanted variation in an independent test set alone as it requires the test set to be normalised with the learning set in a transductive rather than inductive approach (Hughey and Butte, 2015). This is a clear example where over-fitting and over-optimistic results can be an issue, even when a test set is considered.

In this study, we propose a novel Multivariate INTegrative method, *MINT*, that is the first approach of its kind to *simultaneously*, account for unwanted (study) variation, classify samples and identify key discriminant variables when integrating independent data sets. *MINT* predicts the class of new samples from external studies, which enable a direct assessment of its performance. It also provides insightful graphical outputs to improve interpretation and inspect each study during the integration process. Taking advantage of the extensive MAQC project that has been carefully designed to assess unwanted sources of variation, we first validated MINT on a subset of this study. We first confirmed the validity of MINT by taking advantage of the extensive MicroArray Quality Control (MAQC) project that has been carefully designed to assess unwanted sources of variation. We then combined microarray and RNA-seq experiments to discriminate three classes of human cell types (human Fibroblasts (Fib), human Embryonic Stem Cells (hESC) and human induced Pluripotent Stem Cells (hiPSC)) and four classes of breast cancer (subtype *Basal, HER2, Luminal A* and *Luminal B* (Parker *et al.*, 2009)). The genes selected by MINT included existing and novel biomarkers with high potential to improve understanding of the differences among the classes. The resulting *MINT* gene signatures demonstrated excellent accuracy and reproducibility on external test sets when compared to multiple sequential approaches.

2 Results

2.1 Validation of the *MINT* approach to identify signatures agnostic to batch effect

The MAQC project processed technical replicates of four well-characterised biological samples A, B, C and D across three platforms. Thus, we assumed that genes that are differentially expressed (DEG) in every single platform are true positive. We primarily focused on identifying biomarkers that discriminate C vs D, and report the results of A vs B in the Supplemental Material S4.1. Differential expression

analysis of C vs D was conducted on each of the three microarray platforms using ANOVA, showing an overlap of 1,385 DEG (FDR $< 10^{-3}$, Benjamini and Hochberg 1995), which we considered as true positive. This corresponded to 62.6% of all DEG for Illumina, 30.5% for AffyHuGene and 21.0% for AffyPrime (Figure S3). We observed that conducting a differential analysis on the concatenated data from the three microarray platforms without accommodating for batch effects resulted in 691 DEG, of which only 56% (387) were true positive genes. This implies that the remaining 44% (304) of these genes were false positive, and hence were not DE in at least one study. The high percentage of false positive was explained by a Principal Component Analysis (PCA) sample plot that showed samples clustering by platforms (Figure S3), which confirmed that the major source of variation in the combined data was attributed to platforms rather than cell types.

MINT selected a single gene, BCAS1, to discriminate the two biological classes C and D. BCAS1 was a true positive gene, as part of the common DEG, and was ranked 1 for Illumina, 158 for AffyPrime and 1,182 for AffyHuGene. Since the biological samples C and D are very different, the selection of one single gene by MINT was not surprising. To further investigate the performance of MINT, we expanded the number of genes selected by MINT, by decreasing its sparsity parameter (see Methods), and compared the overlap between this larger MINT signature and the true positive genes. We observed an overlap of 100% for a MINT signature of size 100, and an overlap of 89% for a signature of size $1,385$, which is the number of common DEG identified previously. The high percentage of true positive selected by MINT demonstrates its ability to identify a signature agnostic to batch effect.

2.2 Limitations of common meta-analysis and integrative approaches

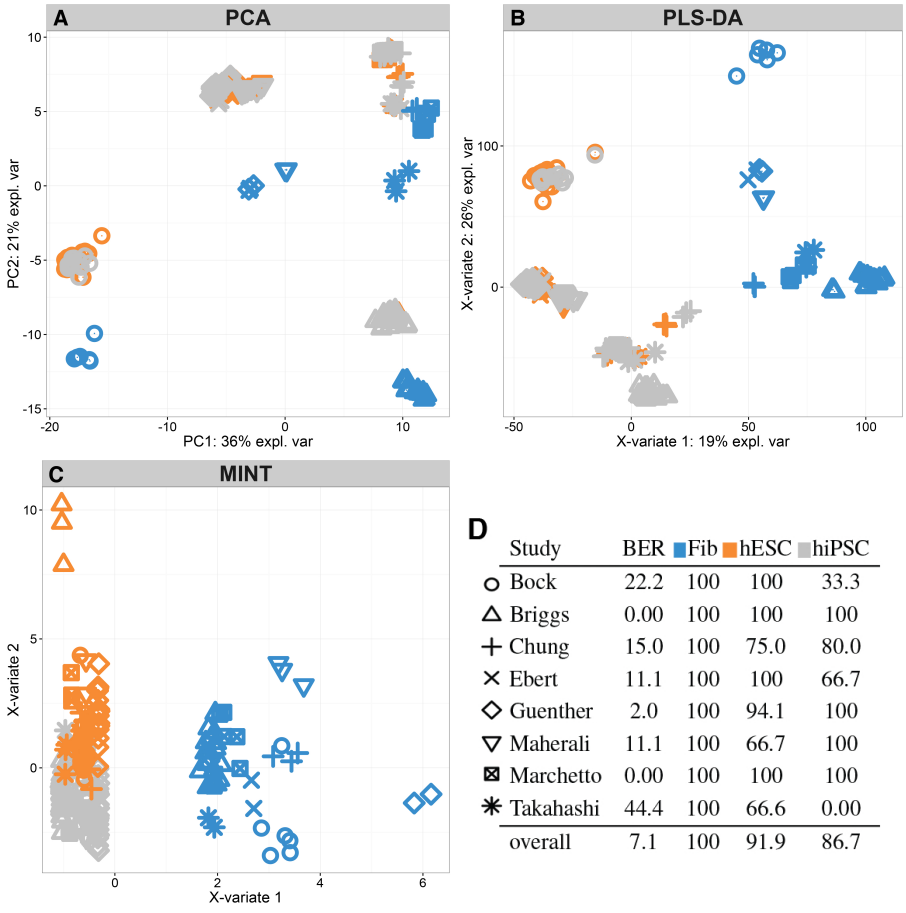

Figure 1: Stem cell study. (A) PCA on the concatenated data: a greater study variation than a cell type variation is observed. (B) PLSDA on the concatenated data clustered Fibroblasts only. (C) *MINT* sample plot shows that each cell type is well clustered, (D) *MINT* performance: BER and classification accuracy for each cell type and each study.

A meta-analysis of eight stem cell studies, each including three cell types (Table 1, stem cell training set), highlighted a small overlap of DEG lists obtained from the analysis of each separate study (FDR $< 10^{-5}$, ANOVA, Supplemental Information S5.2). Indeed, the Takahashi study that declared only 24 DEG limited the overlap between all eight studies to only 5 DEG. This represents a major limitation of merging pre-analysed gene lists as the concordance between DEG lists decreases when the number of studies increases.

One alternative to meta-analysis is to perform an integrative analysis by concatenating all eight studies. Similarly to the MAQC analysis, we first observed that the major source of variation in the combined data was attributed to study rather than cell type (Figure 1A). A PLS-DA was used to discriminate the samples according to their cell types, and it showed a strong study variation (Figure 1B), despite being a supervised analysis. Compared to unsupervised PCA (Figure 1A), the study effect is reduced for the fibroblast cells, but still present for the similar cell types hESC and hiPSC. We reached similar conclusions when analysing the breast cancer data (Supplemental Information S6.2).

2.3 *MINT* outperforms state-of-the-art methods

We compared the classification accuracy of *MINT* to sequential methods where batch removal methods were applied prior to classification methods. In both stem cell and breast cancer studies, MINT led to the best accuracy on the training set, and demonstrated the best reproducibility of the classification model on the test set (lowest Balanced Error Rate, BER, Figure 2, S12). In addition, MINT consistently ranked first as the best performing method, followed by ComBat+sPLSDA with an average rank of 4.5 (Figure S4).

On the stem cell data, we found that fibroblasts were the easiest to classify for all methods, including those that do not accommodate unwanted variation (PLS-DA, sPLS-DA and RF, Figure S6). Classifying hiPSC vs hESC proved more challenging for all methods, leading to a substantially lower classification accuracy than fibroblasts.

The analysis of the breast cancer data (excluding PAM50 genes) showed that methods that do not accommodate unwanted variation were able to rightly classify most of the samples from the training set, but failed at classifying any of the four subtypes on the external test set. As a consequence, all samples were predicted as *LumB* with PLS-DA and sPLS-DA, or *Basal* with RF (Figure S12). Thus, RF gave a satisfactory performance on the training set (BER = 18.5), but a poor performance on the test set (BER= 75).

Additionally, we observed that the biomarker selection process substantially improved classification accuracy. On the stem cell data, LM+sPLSDA and *MINT* outperformed their non sparse counterparts LM+PLSDA and mgPLS (Figure 2, BER of 9.8 and 7.1 vs 20.8 and 11.9), respectively.

Finally, *MINT* was largely superior in terms of computational efficiency. The training step on the stem cell data which includes 210 samples and $13,313$ was run in 1 second, compared to 8 seconds with the second best performing method ComBat+sPLS-DA (2013 MacNook Pro 2.6Ghz, 16Gb memory). The popular method ComBat took $7.1s$ to run, and sPLS-DA $0.9s$. The training step on the breast cancer data that includes $2,817$ samples and $15,755$ genes was run in $37s$ for MINT and $71.5s$ for ComBat($30.8s$)+sPLS-DA($40.6s$).

2.4 Study-specific outputs with *MINT*

One of the main challenges when combining independent studies is to assess the concordance between studies. During the integration procedure, MINT proposes not only individual performance accuracy assessment, but also insightful graphical outputs that are study-specific and can serve as Quality Control step to detect outlier studies. One particular example is the Takahashi study from the stem cell data, whose poor performance (Figure 1D) was further confirmed on the study-specific outputs (Figure S9). Of note, this study was the only one generated through Agilent technology and its sample size only accounted for 4.2% of the training set.

The sample plots from each individual breast cancer data set showed the strong ability of MINT to discriminate the breast cancer subtypes while integrating data sets generated from disparate transcriptomics platforms, microarrays and RNA-sequencing (Figure 3A-C). Those data sets were all differently pre-processed, and yet MINT was able to model an overall agreement between all studies; *MINT* successfully built a space based on a handful of genes in which samples from each study are discriminated in a

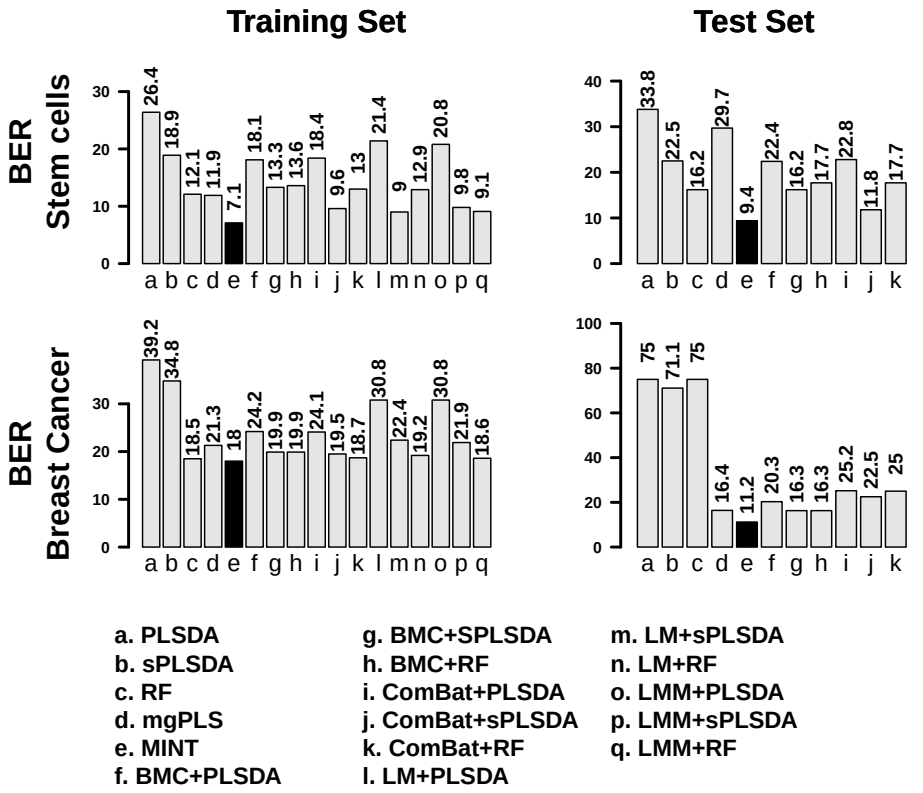

Figure 2: Classification accuracy for both training and test set for the stem cells and breast cancer studies (excluding PAM50 genes). The classification Balanced Error Rates (BER) are reported for all sixteen methods compared with MINT (in black).

homogenous manner.

2.5 *MINT* gene signature identified promising biomarkers

MINT is a multivariate approach that builds successive components to discriminate categories of an outcome. On the stem cell data, *MINT* selected 2 and 15 genes on the first two components respectively (Supplemental Information S5.4). The first component clearly segregated the pluripotent cells (fibroblasts) vs the two non-pluripotent cell types (hiPSC and hESC) (Figure 1C, 1D). Those non pluripotent cells were subsequently separated on component two with some expected overlap given the similarities between hiPSC and hESC. The two genes selected by MINT on component 1 were Lin28A and CAR which were both found relevant in the literature. Indeed, Lin28A was shown to be highly expressed in ESCs compared to Fibroblasts (Yu *et al.*, 2007; Tsialikas and Romer-Seibert, 2015) and CAR has been associated to pluripotency (Krivega *et al.*, 2014). Finally, despite the high heterogeneity of hiPSC cells included in this study, MINT gave a high accuracy for hESC and hiPSC on independent test sets (93.9% and 77.9% respectively, Figure S6), suggesting that the 15 genes selected by MINT on component 2 have a high potential to explain the differences between those cell types (Table S5).

On the breast cancer study, we performed two analyses which either included or discarded the PAM50 genes that were used to define the four cancer subtypes *Basal, HER2, Luminal A* and *Luminal B* (Parker *et al.*, 2009). In the first analysis, we aimed to assess the ability of MINT to specifically identify the PAM50 key driver genes. *MINT* successfully recovered 37 of the 48 PAM50 genes present in the data (77%) on the first three components (7, 20 and 10 respectively). The overall signature included 30, 572 and 636 genes on each component, i.e. 7.8% of the total number of genes in the data. The performance of *MINT* (BER of 17.8 on the training set and 11.6 on the test set) was superior than when performing a PLS-DA on the PAM50 genes only (BER of 20.8 on the training set and a very high 75 on the test set). This result shows that the genes selected by MINT offer a complementary characterisation to the PAM50

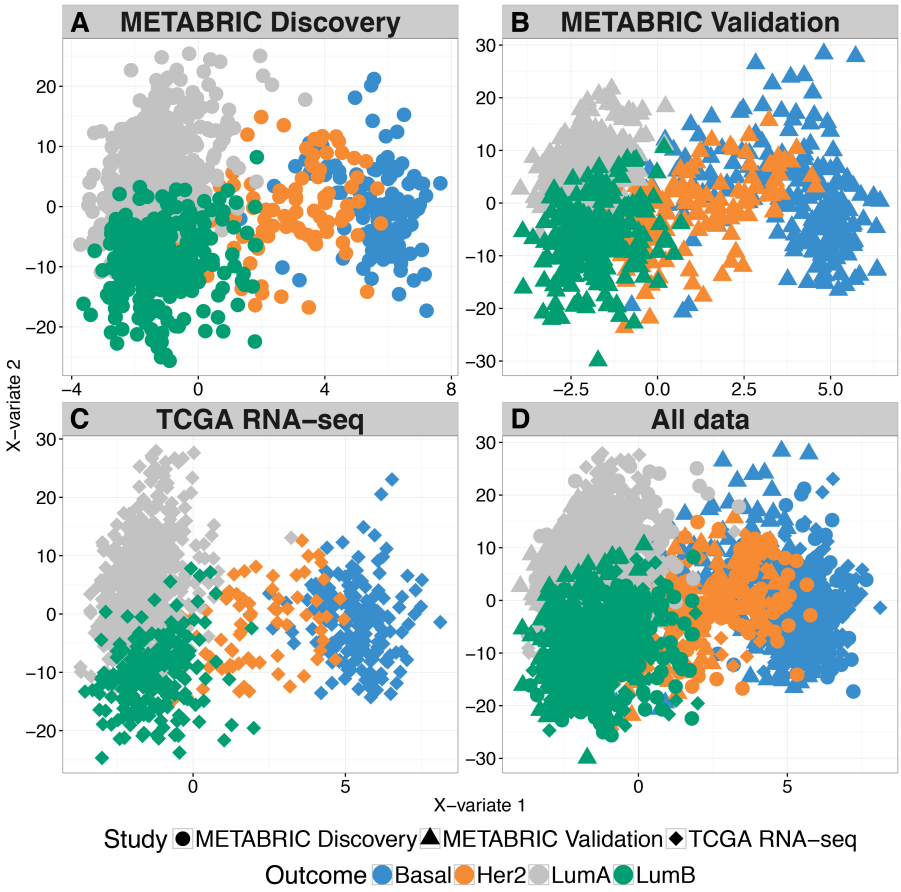

E

Study	BER	Basal	Her2	LumA	LumB
METABRIC Discovery	14.5	91.5	80.5	94.2	75.7
METABRIC Validation	22.3	77.0	65.4	93.3	75.0
TCGA RNA-seq	15.7	98.4	70.0	95.8	72.8
overall	18.0	88.1	70.6	94.7	74.6

Figure 3: *MINT* study-specific sample plots showing the projection of samples from A) METABRIC Discovery, (B) METABRIC Validation and (C) TCGA-RNA-seq experiments, in the same subspace spanned by the first two MINT components. The same subspace is also used to plot the (D) overall (integrated) data. (E) Balanced Error Rate and classification accuracy for each study and breast cancer subtype from the MINT analysis.

genes.

In the second analysis, we aimed to provide an alternative signature to the PAM50 genes by ommitting them from the analysis. *MINT* identified 11, 272 and 253 genes on the first three components respectively (Table S6, S6-2 and Figure S13-S14). The genes selected on the first component gradually differentiated *Basal, HER2* and *Luminal A/B*, while the second component genes further differentiated *Luminal A* from *Luminal B* (Figure 3D). The classification performance was similar in each study (Figure 3E), highlighting an excellent reproducibility of the biomarker signature across cohorts and platforms.

Among the 11 genes selected by MINT on the first component, GATA3 is a transcription factor that regulates luminal epithelial cell differentiation in the mammary glands (Kouros-Mehr *et al.*, 2006; Asselin-Labat *et al.*, 2007), it was found to be implicated in luminal types of breast cancer (Jiang *et al.*, 2014) and was recently investigated for its prognosis significance (McCleskey *et al.*, 2015). The MYB-protein plays an essential role in Haematopoiesis and has been associated to Carcinogenesis (Vargova *et al.*, 2011; Khan *et al.*, 2015). Other genes present in our *MINT* gene signature include XPB1 (Chen *et al.*, 2014), AGR3 (Garczyk *et al.*, 2015), CCDC170 (Yamamoto-Ibusuki *et al.*, 2015) and TFF3 (May and Westley, 2015)

that were reported as being associated with breast cancer. The remaining genes have not been widely associated with breast cancer. For instance, TBC1D9 has been described as over expressed in cancer patients (Andres *et al.*, 2013, 2014). DNALI1 was first identified for its role in breast cancer in Parris *et al.* (2010) but there was no report of further investigation. Although AFF3 was never associated to breast cancer, it was recently proposed to play a pivotal role in adrenocortical carcinoma (Lefevre *et al.*, 2015). It is worth noting that these 11 genes were all included in the 30 genes previously selected when the PAM50 genes were included, and are therefore valuable candidates to complement the PAM50 gene signature as well as to further characterise breast cancer subtypes.

3 Discussion

The issue of unwanted systematic variation resulting from integrating data generated by different microarray platforms has received growing interest from the biological and computational community, and several efficient methods were proposed (Gagnon-Bartsch and Speed, 2012; Johnson *et al.*, 2007; Sims *et al.*, 2008; Listgarten *et al.*, 2010; Lê Cao *et al.*, 2014). When studies aim to classify samples, the common approach is to sequentially apply batch effect removal techniques as a pre-processing step before performing classification. Such approach may lead to over-optimistic results due to either the use of transductive modelling (e.g. prediction based on ComBat-normalised data, Hughey and Butte 2015) or the lack of a test set that is neither normalised nor pre-processed with the training set. To address this crucial issue, we proposed a new Multivariate INTegrative method, MINT, that simultaneously corrects for batch effects, classifies samples and selects a subset of the most discriminant biomarkers across studies. MINT builds a subspace in which independent studies display a homogeneous discrimination of the outcome, thus providing sample plot and classification performance specific to each study (Figure 3). Among the compared methods, MINT was found to be the fastest and most accurate method to integrate and classify data from different microarray and RNA-seq platforms. In addition, MINT is not limited to a classification framework and was extended to a regression framework when Y contains a single or multiple continuous outcomes (multiple multivariate regression, Supplemental Information S2).

Integrative approaches as MINT are necessary when combining multiple studies of complex data in order to limit spurious conclusions from any downstream analysis. Current non-integrative methods displayed a high level of false positive (44% on MAQC data) and exhibited very poor prediction accuracy (PLS-DA, sPLS-DA and RF, Figure 2). Therefore, batch effects assessment should be a compulsory preliminary step. For example PCA can help assessing whether the technical variability is higher than the biological variability (Figure 1A). Failure to do so might result in satisfactory classification accuracy on a training set but very poor accuracy on an independent test set, as we observed with RF on the breast cancer data (Figure 2). Thus, on the training test RF was ranked second most accurate after MINT, but was ranked the worse out of seventeen methods compared on the test set. This stresses the utmost importance of using an external test set to assess the performance of a classification method and avoid spurious conclusions.

The MicroArray Quality Control (MAQC) project provided an excellent case study to assess the ability of *MINT* to identify a relevant gene signature while simultaneously removing batch effects in a classification framework. MINT selected a high percentage of true positive genes, demonstrating successful data integration by selecting key discriminant variables that were also differentially expressed in each experiment. Regarding the stem cells and breast cancer data, MINT displayed the best classification accuracy on the training sets and the best prediction accuracy on the testing sets, when compared to sixteen sequential procedures (Figure 2). These two results implies that the discriminant variables identified by MINT are of great biological relevance, in addition to being highly predictive.

On the stem cell data, MINT identified 2 genes LIN28A and CAR, to discriminate pluripotent cells (fibroblasts) against non-pluripotent cells (hiPSC and hESC). Pluripotency is well-documented in the literature and although OCT4 is the main known marker for undifferentiated cells (Rosner *et al.*, 1990; Schöler *et al.*, 1990; Niwa *et al.*, 2000; Matin *et al.*, 2004), it was not selected by MINT on the first component. Further investigation showed that LIN28A and CAR were ranked higher than OCT4 in the DEG list obtained on the concatenated data (Lin28A pval=1.5e-40, CAR pval = 5.2e-43, OCT4 pval = 4.3e-29, two-sided Welch's t-test). OCT4 was therefore found differentially expressed and should not be discarded as a marker of pluripotency, however our analysis suggests that LIN28A and CAR are highly reproducible markers of differentiated cells, and could potentially substitute or complement OCT4. Further experimen-

tal validation would be required to further assess the potential of LIN28A or CAR as efficient markers.

Several problems arise when integrating data, as we faced with the stem cell and breast cancer studies generated from multiple research groups and different microarray and RNA-seq platforms. First and foremost, sample classification is crucial and needs to be well defined. For instance, the breast cancer subtype classification relied on the PAM50 intrinsic classifier proposed by Parker *et al.* (2009), which is still leads to some controversy. For example Curtis *et al.* (2012) proposed the IC10 classification of ten subtypes of breast cancers. Similarly, the biological definition of hiPSC differs across research groups, which results in poor reproducibility among experiments and makes the integration of stem cell studies a great analytical challenge. We previously raised this issue when developing a novel and robust signature of Mesenchymal stem cells (MSC) as the field had not yet reached a consensus on the definition of a MSC (Rohart *et al.* 2016). In our previous work, 'gold standard' MSC characteristics were defined by our team as the minimum requirements for a cell to be a MSC; then, hundreds of datasets and linked publications were screened to assess whether samples met our criteria. In this present study, however, we trusted the annotation provided by the authors as 'gold standard'. We acknowledge the occurrence of disparities in this process as one research group may have different criteria to call a sample a hiPSC. This situation was previously discussed as a potential reason behind the differences between hiPSC and hESC (Bilic and Belmonte, 2012; Newman and Cooper, 2010). The expertise and exhaustive screening required to homogeneously annotate samples critically hinders the downstream data integration.

The second issue we faced when integrating datasets from different sources is limited access to raw data in public databases. Indeed, each study may have been normalised or pre-processed differently, as in the breast cancer study. The disparity in these crucial processing steps may substantially add to unwanted variation between studies. While MINT gave satisfactory results on the breast cancer data, we highly recommend either seeking raw data, or using high quality databases were each data set is homogeneously pre-processed, for example using background correction, log2- and YuGene-transformation on the stem cell study from the stemformatics resource (Wells *et al.*, 2013).

The last issue pertains to the differences between study and platform effects. PCA plots showed that samples primarily clustered according studies, but within platform types (Figure 1A and Figure S10A), suggesting that the largest source of variation when integrating datasets is experimental platform (75% of the variance in the breast cancer data, Figure S10A). Indeed, and as discussed by Shi *et al.* (2006) on the MAQC project, there exists inherent differences between commercial platforms that greatly magnify unwanted variability. Since platform and study effects are nested, current batch-removal methods and *MINT* dismiss the platform information and model the study effect only. We think that such strategy may be sufficient in most integrative analysis scenarios, as MINT successfully integrated microarray and RNA-seq data on the breast cancer data.

MINT is available through the mixMINT module in the user-friendly mixOmics R-package. Some considerations should be taken into account when applying our method. In order to reduce unwanted systematic variation, the method centers and scales each study as an initial step, similarly to BMC (Sims *et al.*, 2008). Therefore, only studies with a sample size > 3 can be included. In addition, all outcome categories need to be represented in each study in order for *MINT* to be fully efficient.

4 Conclusion

We introduced MINT, a novel Multivariate INTegrative method, that is the first approach to integrate independent transcriptomics studies from different microarray and RNA-seq platforms by *simultaneously*, correcting for batch effects, classifying samples and identifying key discriminant variables. We first validated the ability of MINT to select true positives genes when integrating the MAQC data across different platforms. MINT was then benchmarked against sixteen sequential approaches and showed to be the fastest and most accurate method to discriminate and predict three human cell types (human Fibroblasts, human Embryonic Stem Cells and human induced Pluripotent Stem Cells) and four subtypes of breast cancer (Basal, HER2, Luminal A and Luminal B). The gene signatures identified by MINT included existing and novel biomarkers that can be considered as promising candidates to better characterise phenotypes. MINT is available through the mixMINT module in the mixOmics R-package.

5 Methods

We use the following notations. Let X denote a data matrix of size N observations (rows) $\times$ P variables (e.g. gene expression levels, in columns) and Y a dummy matrix indicating each sample class membership of size N observations (rows) $\times$ K categories outcome (columns). We assume that the data are partitioned into M groups corresponding to each independent study m: $\{(X^{(1)}, Y^{(1)}), \ldots, (X^{(M)}, Y^{(M)})\}$ so that $\sum_{m=1}^{M} n_m = N$, where n_m is the number of samples in group m, see Figure 4. Each variable from the data set $X^{(m)}$ and $Y^{(m)}$ is centered and has unit variance. We write X and Y the concatenation of all $X^{(m)}$ and $Y^{(m)}$, respectively. For $n \in \mathbb{N}$, we denote for all $a \in \mathbb{R}^n$ its ℓ^1 norm $||a||_1 = \sum_1^n |a_j|$ and its ℓ^2 norm $||a||_2 = (\sum_1^n a_j^2)^{1/2}$ and $|a|_+$ the positive part of a. For any matrix we denote by $^\top$ its transpose.

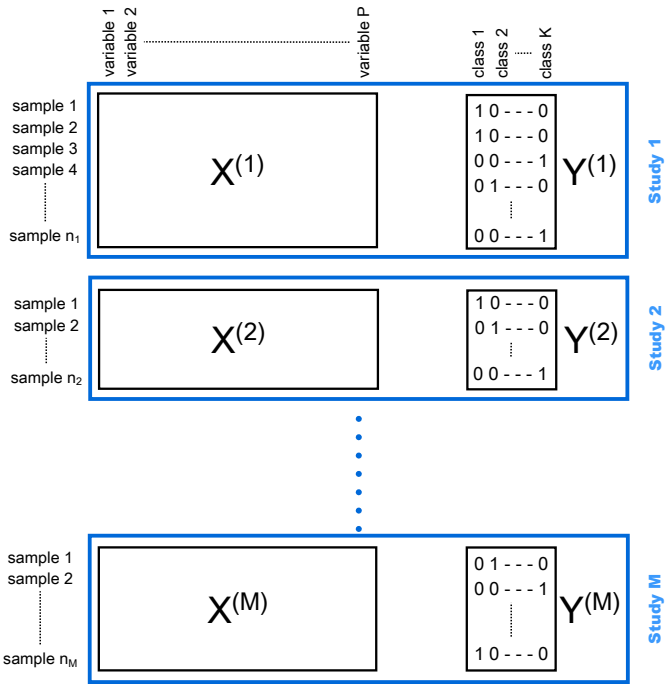

Figure 4: Experimental design of *MINT*, combining M independent studies $X^{(m)}, Y^{(m)}$, where $X^{(m)}$ is a data matrix of size n_m observations (rows) $\times$ P variables (e.g. gene expression levels, in columns) and $Y^{(m)}$ is a dummy matrix indicating each sample class membership of size n_m observations (rows) $\times$ K categories outcome (columns).

5.1 PLS-based classification methods to combine independent studies

PLS approaches have been extended to classify samples Y from a data matrix X by maximising a formula based on their covariance. Specifically, latent components are built based on the original X variables to summarise the information and reduce the dimension of the data while discriminating the Y outcome. Samples are then projected into a smaller space spanned by the latent component. We first detail the classical PLS-DA approach and then describe mgPLS, a PLS-based model we previously developed to model a group (study) structure in X.

PLS-DA. Partial Least Squares Discriminant Analysis (Barker and Rayens, 2003) is an extension of PLS for a classification frameworks where Y is a dummy matrix indicating sample class membership. In our study, we applied PLS-DA as an integrative approach by naively concatenating all studies. Briefly, PLS-DA is an iterative method that constructs H successive artificial (latent) components $t_h = X_h a_h$ and $u_h = Y_h b_h$ for $h = 1, .., H$, where the h^{th} component t_h (respectively u_h) is a linear combination of the X (Y) variables. H denotes the dimension of the PLS-DA model. The weight coefficient vector a_h (b_h) is the loading vector that indicates the *importance* of each variable to define the component. For each dimension

$h = 1, \ldots, H$ PLS-DA seeks to maximize

$$\max_{||a_h||_2=||b_h||_2=1} cov(X_h a_h, Y_h b_h), \quad (1)$$

where X_h, Y_h are residual matrices (obtained through a *deflation step*, as detailed in Lê Cao *et al.* 2011). The PLS-DA algorithm is described in Supplemental Information S1. The PLS-DA model assigns to each sample i a pair of H scores (t_h^i, u_h^i) which effectively represents the projection of that sample into the X- or Y- space spanned by those PLS components. As $H << P$, the projection space is small, allowing for dimension reduction as well as insightful sample plot representation (e.g. graphical outputs in Section 2). While PLS-DA ignores the data group structure inherent to each independent study, it can give satisfactory results when the between groups variance is smaller than the within group variance or when combined with extensive data subsampling to account for systematic variation across platforms (Rohart *et al.*, 2016).

mgPLS. Multi-group PLS is an extension of the PLS framework we recently proposed to model grouped data (Eslami *et al.*, 2013, 2014), which is relevant for our particular case where the groups represent independent studies. In mgPLS, the PLS-components of each group are constraint to be built based on the same loading vectors in X and Y. These *global* loading vectors thus allow the samples from each group or study to be projected in the same common space spanned by the PLS-components. We extended the original unsupervised approach to a supervised approach by using a dummy matrix Y as in PLS-DA to classify samples while modelling the group structure. For each dimension $h = 1, \ldots, H$ mgPLS-DA seeks to maximize

$$\max_{||a_h||_2=||b_h||_2=1} \sum_{m=1}^{M} n_m cov(X_h^{(m)} a_h, Y_h^{(m)} b_h), \quad (2)$$

where a_h and b_h are the global loadings vectors common to all groups, $t_h^{(m)} = X_h^{(m)} a_h$ and $u_h^{(m)} = Y_h^{(m)} b_h$ are the group-specific (partial) PLS-components, and $X_h^{(m)}$ and $Y_h^{(m)}$ are the residual (deflated) matrices. The global loadings vectors (a_h, b_h) and global components ($t_h = X_h a_h$, $u_h = Y_h b_h$) enable to assess overall classification accuracy, while the group-specific loadings and components provide powerful graphical outputs for each study that is integrated in the analysis. Global and group-specific components and loadings are represented in Figure S1. The next development we describe below is to include internal variable selection in mgPLS-DA for large dimensional data sets.

5.2 *MINT*

Our novel multivariate integrative method *MINT* *simultaneously* integrates independent studies and selects the most discriminant variables to classify samples and predict the class of new samples. MINT seeks for a common projection space for all studies that is defined on a small subset of discriminative variables and that display an analogous discrimination of the samples across studies. The identified variables share common information across all studies and therefore represent a reproducible signature that helps characterising biological systems. *MINT* further extends mgPLS-DA by including a ℓ^1-penalisation on the global loading vector a_h to perform variable selection. For each dimension $h = 1, \ldots, H$ the *MINT* algorithm seeks to maximize

$$\max_{||a_h||_2=1} \sum_{m=1}^{M} n_m cov(X_h^{(m)} a_h, Y_h^{(m)} b_h) + \lambda_h ||a_h||_1, \quad (3)$$

where in addition to the notations from equation (2), λ_h is a non negative parameter that controls the amount of shrinkage on the global loading vectors a_h and thus the number of non zero weights. Similarly to Lasso (Tibshirani, 1996) or sparse PLS-DA (Lê Cao *et al.*, 2011), the added ℓ^1 penalisation in *MINT* improves interpretability of the PLS-components that are now defined only on a set of selected biomarkers from X (with non zero weight) that are identified in the linear combination $X_h^{(m)} a_h$. The ℓ^1 penalisation in effectively solved in the *MINT* algorithm using soft-thresholding (see pseudo Algorithm 1).

5.3 Class prediction and parameters tuning with *MINT*

MINT centers and scales each study from the training set, so that each variable has mean 0 and variance 1, similarly to any PLS methods. Therefore, a similar pre-processing needs to be applied on test sets. If a

Algorithm 1 *MINT*

We denote $\forall\ 1 \leq m \leq M, X_1^{(m)} = X^{(m)}$, $Y_1^{(m)} = Y^{(m)}$, $X^{(m)} = X$ and $Y^{(m)} = Y$, where X and Y are centered and scaled.
For $h < H$, choose λ_h and an initial value for a_h with $||a_h||_2 = 1$,
repeat
  $t_h^{(m)} \leftarrow X_h^{(m)} a_h$ ▷ partial components
  $t_h \leftarrow X_h a_h$ ▷ global components
  $b_h^{(m)} \leftarrow (Y_h^{(m)})^\top t_h^{(m)}$ ▷ partial loadings
  $b_h \leftarrow (\sum_{m=1}^M b_h^{(m)})/||\sum_{m=1}^M b_h^{(m)}||_2$ ▷ global loadings
  $u_h^{(m)} \leftarrow Y_h^{(m)} b_h$ ▷ partial components
  $a_h^{(m)} \leftarrow (X_h^{(m)})^\top u_h^{(m)}$ ▷ partial loadings
  $a_h \leftarrow (\sum_{m=1}^M a_h^{(m)})/||\sum_{m=1}^M a_h^{(m)}||_2$ ▷ global loadings
  $a_h \leftarrow sign(a_h)(|a_h| - \lambda_h)_+$ ▷ soft thresholding
until convergence of a_h and b_h.
$P \leftarrow I - t_h(t_h^\top t_h)^{-1} t_h^\top$, where I = identity matrix of $\mathbb{R}^N$
$X_{h+1} \leftarrow PX_h$ and $Y_{h+1} \leftarrow PY_h$ ▷ deflation

test sample belongs to a study that is part of the training set, then we apply the same scaling coefficients as from the training study. If the test study is completely independent, then it is centered and scaled separately.

After scaling the test samples, the prediction framework of PLS is used to estimate the dummy matrix Y_{test} of an independent test set X_{test} (Tenenhaus, 1998), where each row in Y_{test} sums to 1, and each column represents a class of the outcome. A class membership is assigned (predicted) to each test sample by using the maximal distance, as described in Lê Cao *et al.* (2011). It consists in assigning the class with maximal positive value in Y_{test}.

The main parameter to tune in MINT is the penalty λ_h for each PLS-component h, which is usually performed using Cross-Validation (CV). In practice, the parameter λ_h can be equally replaced by the number of variables to select on each component, which is our preferred user-friendly option. The assessment criterion in the CV can be based on the proportion of misclassified samples, proportion of false or true positives, or, as in our case, the balanced error rate (BER). BER is calculated as the averaged proportion of wrongly classified samples in each class and weights up small sample size classes. We consider BER to be a more objective performance measure than the overall misclassification error rate when dealing with unbalanced classes. *MINT* tuning is computationally efficient as it takes advantage of the group data structure in the integrative study. We used a "Leave-One-Group-Out Cross-Validation (LOGOCV)", which consists in performing CV where group or study m is left out only once $m = 1, \ldots, M$. LOGOCV realistically reflects the true case scenario where prediction is performed on independent external studies based on a reproducible signature identified on the training set. Finally, the total number of components H in *MINT* is set to $K - 1$, K = number of classes, similar to PLS-DA and ℓ^1 penalised PLS-DA models (Lê Cao *et al.*, 2011).

5.4 Case studies

We demonstrate the ability of *MINT* to identify the true positive genes on the MAQC project, then highlight the strong properties of our method to combine independent data sets in order to identify reproducible and predictive gene signatures on two other biological studies.

The MicroArray Quality Control (MAQC) project. The extensive MAQC project focused on assessing microarray technologies reproducibility in a controlled environment (Shi *et al.*, 2006). Two reference samples, RNA samples Universal Human Reference (UHR) and Human Brain Reference (HBR) and two mixtures of the original samples were considered. Technical replicates were obtained from three different array platforms -Illumina, AffyHuGene and AffyPrime- for each of the four biological samples A (100% UHR), B (100% HBR), C (75% UHR, 25% HBR) and D (25%UHR and 75% HBR). Data were downloaded from Gene Expression Omnibus (GEO) - GSE56457. In this study, we focused on identifying biomarkers that discriminate A vs B and C vs D. The experimental design is referenced in Table S1.

Stem cells. We integrated 15 transcriptomics microarray datasets to classify three types of human cells: human Fibroblasts (Fib), human Embryonic Stem Cells (hESC) and human induced Pluripotent Stem Cells (hiPSC). As there exists a biological hierarchy among these three cell types, two sub-classification problems are of interest in our analysis, which we will address simultaneously with *MINT*. On the one hand, differences between pluripotent (hiPSC and hESC) and non-pluripotent cells (Fib) are well-characterised and are expected to contribute to the main biological variation. Our first level of analysis will therefore benchmark *MINT* against the gold standard in the field. On the other hand, hiPSC are genetically reprogrammed to behave like hESC and both cell types are commonly assumed to be alike. However, differences have been reported in the literature (Bilic and Belmonte, 2012; Chin *et al.*, 2009; Newman and Cooper, 2010), justifying the second and more challenging level of classification analysis between hiPSC and hESC. We used the cell type annotations of the 342 samples as provided by the authors of the 15 studies. The stem cell dataset provides an excellent showcase study to benchmark *MINT* against existing statistical methods to solve a rather ambitious classification problem.
Each of the 15 studies was assigned to either a training or test set. Platforms uniquely represented were assigned to the training set and studies with only one sample in one class were assigned to the test set. Remaining studies were randomly assigned to training or test set. Eventually, the training set included eight datasets (210 samples) derived on five commercial platforms and the independent test set included the remaining seven datasets (132 samples) derived on three platforms (Table 1 and Table S3).
The pre-processed files were downloaded from the `www.stemformatics.org` collaborative platform (Wells *et al.*, 2013). Each dataset was background corrected, log2 transformed, YuGene normalized and mapped from probes ID to Ensembl ID as previously described in Lê Cao *et al.* (2014), resulting in 13 313 unique Ensembl gene identifiers. In the case where datasets contained multiple probes for the same Ensembl ID gene, the highest expressed probe was chosen as the representative of that gene in that dataset. The choice of YuGene normalisation was motivated by the need to normalise each sample independently rather than as a part of a whole study (e.g. existing methods ComBat (Johnson *et al.*, 2007), quantile normalisation (RMA, Bolstad *et al.* 2003)), to effectively limit over-fitting during the CV evaluation process.

Experiment	Platform	Fib	hESC	hiPSC
Bock	Affymetrix HT-HG-U133A	6	20	12
Briggs	Illumina HumanHT-12 V4	18	3	30
Chung	Affymetrix HuGene-1.0-ST V1	3	8	10
Ebert	Affymetrix HG-U133 Plus2	2	5	3
Guenther	Affymetrix HG-U133 Plus2	2	17	20
Maherali	Affymetrix HG-U133 Plus2	3	3	15
Marchetto	Affymetrix HuGene-1.0-ST V1	6	3	12
Takahashi	Agilent SurePrint G3 GE 8x60K	3	3	3
Total training set	5 platforms	43	62	105
Andrade	Affymetrix HuGene-1.0-ST V1	3	6	15
Hu	Affymetrix HG-U133 Plus2	1	5	12
Kim	Affymetrix HG-U133 Plus2	1	1	3
Loewer	Affymetrix HG-U133 Plus2	4	2	7
Si-Tayeb	Affymetrix HG-U133 Plus2	3	6	6
Vitale	Illumina HumanHT-12 V4	8	3	18
Yu	Affymetrix HG-U133 Plus2	2	10	16
Total test set	3 platforms	22	33	77

Table 1: Stem cell experimental design. A total of 15 studies were analysed, including three human cell types, human Fibroblasts (Fib), human Embryonic Stem Cells (hESC) and human induced Pluripotent Stem Cells (hiPSC) across five different types of microarray platforms. Eight studies from five microarray platforms were considered as a training set and seven independent studies from three of the five platforms were considered as a test set.

Breast Cancer. We combined whole-genome gene-expression data from two cohorts from the Molecular Taxonomy of Breast Cancer International Consortium project (METABRIC, Curtis *et al.* (2012) and of two cohorts from the Cancer Genome Atlas (TCGA, Cancer Genome Atlas Network and others (2012)) to classify the intrinsic subtypes *Basal, HER2, Luminal A* and *Luminal B*, as defined by the PAM50 signature

(Parker *et al.*, 2009). The METABRIC cohorts data were made available upon request, and were processed by Curtis *et al.* (2012). TCGA cohorts are gene-expression data from RNA-seq and microarray platforms. RNA-seq data were normalised using Expectation Maximisation (RSEM) and percentile-ranked gene-level transcription estimates. The microarray data were processed as described in Cancer Genome Atlas Network and others (2012).

The training set consisted in three cohorts (TCGA RNA-seq and both METABRIC microarray studies), including the expression levels of 15 803 genes on 2 814 samples; the test set included the TCGA microarray cohort with 254 samples (Table 2) Two analyses were conducted, which either included or discarded the PAM50 genes from the data. The first analysis aimed at recovering the PAM50 genes used to classify the samples. The second analysis was performed on 15, 755 genes and aimed at identifying an alternative signature to the PAM50.

Experiment	Platform	Basal	Her2	LumA	LumB
METABRIC Discovery	Illumina HT-12 v3	118	87	466	268
METABRIC Validation	Illumina HT-12 v3	213	153	255	224
TCGA RNA-seq	illumina HiSeq 2000	188	80	549	213
Total training set	2 platforms	519	320	1270	705
TCGA microarray	Agilent custom 244K	57	31	99	67
Total test set	1 platform	57	31	99	67

Table 2: Experimental design of four breast cancer cohorts including 4 cancer subtypes: *Basal, HER2, Luminal A* (LumA) and *Luminal B* (LumB).

5.5 Performance comparison with sequential classification approaches

We compared *MINT* with sequential approaches that combine batch-effect removal approaches with classification methods. As a reference, classification methods were also used on their own on a naive concatenation of all studies. Batch-effect removal methods included Batch Mean-Centering (BMC, Sims *et al.* 2008), ComBat (Johnson *et al.*, 2007), linear models (LM) or linear mixed models (LMM), and classification methods included PLS-DA, sPLS-DA (Lê Cao *et al.*, 2011), mgPLS (Eslami *et al.*, 2013, 2014) and Random forests (RF, Breiman 2001). For LM and LMM, linear models were fitted on each gene and the residuals were extracted as a batch-corrected gene expression (Whitcomb *et al.*, 2010; Rohart *et al.*, 2014). The study effect was set as a fixed effect with LM or as a random effect with LMM. No sample outcome (e.g. cell-type) was included. Prediction with ComBat normalised data were obtained as described in Hughey and Butte (2015). In this study, we did not include methods that require extra information -as control genes with RUV-2 (Gagnon-Bartsch and Speed, 2012)- and methods that are not widely available to the community as LMM-EH (Listgarten *et al.*, 2010). Classification methods were chosen so as to simultaneously discriminate all classes. With the exception of sPLS-DA, none of those methods perform internal variable selection. The multivariate methods PLS-DA, mgPLS and sPLS-DA were run on $K - 1$ components, sPLS-DA was tuned using 5-fold CV on each component. All classification methods were combined with batch-removal method with the exception of mgPLS that already includes a study structure in the model.

MINT and PLS-DA-like approaches use a prediction threshold based on distances (see Section 5.3) that optimally determines class membership of test samples, and as such do not require receiver operating characteristic (ROC) curves and area under the curve (AUC) performance measures. In addition, those measures are limited to binary classification which do not apply for our stem cell and breast cancer multiclass studies. Instead we use Balanced classification Error Rate to objectively evaluate the classification and prediction performance of the methods for unbalanced sample size classes (Section 5.2). Classification accuracies for each class were also reported.

Acknowledgements

This project was partly funded by the ARC Discovery grant project DP130100777 (2013-2015), the Australian Cancer Research Foundation for the Diamantina Individualised Oncology Care Centre at UQDI (FR), and the National Health and Medical Research Council (NHMRC) Career Development fellowship APP1087415 (KALC).

References

Andres, S. A., Brock, G. N., and Wittliff, J. L. (2013). Interrogating differences in expression of targeted gene sets to predict breast cancer outcome. *BMC cancer*, **13**(1), 1.

Andres, S. A., Smolenkova, I. A., and Wittliff, J. L. (2014). Gender-associated expression of tumor markers and a small gene set in breast carcinoma. *The Breast*, **23**(3), 226–233.

Asselin-Labat, M.-L., Sutherland, K. D., Barker, H., Thomas, R., Shackleton, M., Forrest, N. C., Hartley, L., Robb, L., Grosveld, F. G., van der Wees, J., *et al.* (2007). Gata-3 is an essential regulator of mammary-gland morphogenesis and luminal-cell differentiation. *Nature cell biology*, **9**(2), 201–209.

Barker, M. and Rayens, W. (2003). Partial least squares for discrimination. *Journal of chemometrics*, **17**(3), 166–173.

Benjamini, Y. and Hochberg, Y. (1995). Controlling the false discovery rate: a practical and powerful approach to multiple testing. *J. R. Stat. Soc. Ser. B. Stat. Methodol.*, **57**(1), 289–300.

Bilic, J. and Belmonte, J. C. I. (2012). Concise review: Induced pluripotent stem cells versus embryonic stem cells: close enough or yet too far apart? *Stem Cells*, **30**(1), 33–41.

Bolstad, B. M., Irizarry, R. A., Åstrand, M., and Speed, T. P. (2003). A comparison of normalization methods for high density oligonucleotide array data based on variance and bias. *Bioinformatics*, **19**(2), 185–193.

Breiman, L. (2001). Random forests. *Machine Learning*, **45**(1), 5–32.

Cancer Genome Atlas Network and others (2012). Comprehensive molecular portraits of human breast tumours. *Nature*, **490**(7418), 61–70.

Chen, X., Iliopoulos, D., Zhang, Q., Tang, Q., Greenblatt, M. B., Hatziapostolou, M., Lim, E., Tam, W. L., Ni, M., Chen, Y., *et al.* (2014). Xbp1 promotes triple-negative breast cancer by controlling the hif1 [agr] pathway. *Nature*, **508**(7494), 103–107.

Chin, M. H., Mason, M. J., Xie, W., Volinia, S., Singer, M., Peterson, C., Ambartsumyan, G., Aimiuwu, O., Richter, L., Zhang, J., *et al.* (2009). Induced pluripotent stem cells and embryonic stem cells are distinguished by gene expression signatures. *Cell stem cell*, **5**(1), 111–123.

Curtis, C., Shah, S. P., Chin, S.-F., Turashvili, G., Rueda, O. M., Dunning, M. J., Speed, D., Lynch, A. G., Samarajiwa, S., Yuan, Y., *et al.* (2012). The genomic and transcriptomic architecture of 2,000 breast tumours reveals novel subgroups. *Nature*, **486**(7403), 346–352.

Eslami, A., Qannari, E. M., Kohler, A., and Bougeard, S. (2013). Multi-group PLS Regression: Application to Epidemiology. In *New Perspectives in Partial Least Squares and Related Methods*, pages 243–255. Springer.

Eslami, A., Qannari, E. M., Kohler, A., and Bougeard, S. (2014). Algorithms for multi-group PLS. *J. Chemometrics*, **28**(3), 192–201.

Gagnon-Bartsch, J. A. and Speed, T. P. (2012). Using control genes to correct for unwanted variation in microarray data. *Biostatistics*, **13**(3), 539–552.

Garczyk, S., von Stillfried, S., Antonopoulos, W., Hartmann, A., Schrauder, M. G., Fasching, P. A., Anzeneder, T., Tannapfel, A., Ergönenc, Y., Knüchel, R., *et al.* (2015). Agr3 in breast cancer: Prognostic impact and suitable serum-based biomarker for early cancer detection. *PloS one*, **10**(4), e0122106.

Hughey, J. J. and Butte, A. J. (2015). Robust meta-analysis of gene expression using the elastic net. *Nucleic Acids Res.*, **43**(12), e79.

Jiang, Y.-Z., Yu, K.-D., Zuo, W.-J., Peng, W.-T., and Shao, Z.-M. (2014). Gata3 mutations define a unique subtype of luminal-like breast cancer with improved survival. *Cancer*, **120**(9), 1329–1337.

Johnson, W., Li, C., and Rabinovic, A. (2007). Adjusting batch effects in microarray expression data using empirical Bayes methods. *Biostatistics*, **8**(1), 118–27.

Khan, F. H., Pandian, V., Ramraj, S., Aravindan, S., Herman, T. S., and Aravindan, N. (2015). Reorganization of metastamirs in the evolution of metastatic aggressive neuroblastoma cells. *BMC genomics*, **16**(1), 1.

Kim, S., Lin, C.-W., and Tseng, G. C. (2016). Metaktsp: a meta-analytic top scoring pair method for robust cross-study validation of omics prediction analysis. *Bioinformatics*, page btw115.

Kouros-Mehr, H., Slorach, E. M., Sternlicht, M. D., and Werb, Z. (2006). Gata-3 maintains the differentiation of the luminal cell fate in the mammary gland. *Cell*, **127**(5), 1041–1055.

Krivega, M., Geens, M., and Van de Velde, H. (2014). CAR expression in human embryos and hESC illustrates its role in pluripotency and tight junctions. *Reproduction*, **148**(5), 531–544.

Kuhn, M. (2008). Caret package. *Journal of Statistical Software*, **28**(5).

Lazar, C., Meganck, S., Taminau, J., Steenhoff, D., Coletta, A., Molter, C., Y.Weiss-Solis, D., Duque, R., Bersini, H., and Nowé, A. (2012). Batch effect removal methods for microarray gene expression data integration: a survey. *Brief. Bioinform.*, **14**(4), 469–490.

Lê Cao, K. A., Boitard, S., and Besse, P. (2011). Sparse PLS discriminant analysis: biologically relevant feature selection and graphical displays for multiclass problems. *BMC Bioinformatics*, **12**, 253.

Lê Cao, K. A., Rohart, F., McHugh, L., Korm, O., and Wells, C. A. (2014). YuGene: A simple approach to scale gene expression data derived from different platforms for integrated analyses. *Genomics*, **103**, 239–251.

Lefevre, L., Omeiri, H., Drougat, L., Hantel, C., Giraud, M., Val, P., Rodriguez, S., Perlemoine, K., Blugeon, C., Beuschlein, F., *et al.* (2015). Combined transcriptome studies identify aff3 as a mediator of the oncogenic effects of β-catenin in adrenocortical carcinoma. *Oncogenesis*, **4**(7), e161.

Listgarten, J., Kadie, C., Schadt, E. E., and Heckerman, D. (2010). Correction for hidden confounders in the genetic analysis of gene expression. *Proc. Natl. Acad. Sci. U.S.A.*, **107**(38), 16465–16470.

Matin, M. M., Walsh, J. R., Gokhale, P. J., Draper, J. S., Bahrami, A. R., Morton, I., Moore, H. D., and Andrews, P. W. (2004). Specific Knockdown of Oct4 and β2-microglobulin Expression by RNA Interference in Human Embryonic Stem Cells and Embryonic Carcinoma Cells. *Stem Cells*, **22**(5), 659–668.

May, F. E. and Westley, B. R. (2015). Tff3 is a valuable predictive biomarker of endocrine response in metastatic breast cancer. *Endocr. Relat. Cancer*, **22**(3), 465–479.

McCleskey, B. C., Penedo, T. L., Zhang, K., Hameed, O., Siegal, G. P., and Wei, S. (2015). Gata3 expression in advanced breast cancer: prognostic value and organ-specific relapse. *Am J Clin Path*, **144**(5), 756–763.

Newman, A. M. and Cooper, J. B. (2010). Lab-specific gene expression signatures in pluripotent stem cells. *Cell stem cell*, **7**(2), 258–262.

Niwa, H., Miyazaki, J.-i., and Smith, A. G. (2000). Quantitative expression of Oct-3/4 defines differentiation, dedifferentiation or self-renewal of ES cells. *Nat. Genet.*, **24**(4), 372–376.

Parker, J. S., Mullins, M., Cheang, M. C., Leung, S., Voduc, D., Vickery, T., Davies, S., Fauron, C., He, X., Hu, Z., *et al.* (2009). Supervised risk predictor of breast cancer based on intrinsic subtypes. *J. Clin. Oncol.*, **27**(8), 1160–1167.

Parris, T. Z., Danielsson, A., Nemes, S., Kovács, A., Delle, U., Fallenius, G., Möllerström, E., Karlsson, P., and Helou, K. (2010). Clinical implications of gene dosage and gene expression patterns in diploid breast carcinoma. *Clin Cancer Res*, **16**(15), 3860–3874.

Pihur, V., Datta, S., and Datta, S. (2008). Finding common genes in multiple cancer types through meta–analysis of microarray experiments: A rank aggregation approach. *Genomics*, **92**(6), 400–403.

Rohart, F., San Cristobal, M., and Laurent, B. (2014). Selection of fixed effects in high dimensional linear mixed models using a multicycle ecm algorithm. *Computational Statistics & Data Analysis*, **80**, 209–222.

Rohart, F., Mason, E. A., Matigian, N., Mosbergen, R., Korn, O., Chen, T., Butcher, S., Patel, J., Atkinson, K., Khosrotehrani, K., Fisk, N. M., Lê Cao, K., and Wells, C. A. (2016). A molecular classification of human mesenchymal stromal cells. *PeerJ*, **4**, e1845.

Rosner, M. H., Vigano, M. A., Ozato, K., Timmons, P. M., Poirie, F., Rigby, P. W., and Staudt, L. M. (1990). A POU-domain transcription factor in early stem cells and germ cells of the mammalian embryo. *Nature*, **345**(6277), 686–692.

Schöler, H. R., Ruppert, S., Suzuki, N., Chowdhury, K., and Gruss, P. (1990). New type of POU domain in germ line-specific protein Oct-4. *Nature*, **344**(6265), 435–439.

Shi, L., Reid, L. H., Jones, W. D., Shippy, R., Warrington, J. A., Baker, S. C., Collins, P. J., De Longueville, F., Kawasaki, E. S., Lee, K. Y., *et al.* (2006). The microarray quality control (maqc) project shows inter-and intraplatform reproducibility of gene expression measurements. *Nat. Biotechnol.*, **24**(9), 1151–1161.

Sims, A. H., Smethurst, G. J., Hey, Y., Okoniewski, M. J., Pepper, S. D., Howell, A., Miller, C. J., and Clarke, R. B. (2008). The removal of multiplicative, systematic bias allows integration of breast cancer gene expression datasets–improving meta-analysis and prediction of prognosis. *BMC Med Genomics*, **1**(1), 42.

Su, Z., Labaj, P., Li, S., Thierry-Mieg, J., *et al.* (2014). A comprehensive assessment of rna-seq accuracy, reproducibility and information content by the sequencing quality control consortium. *Nat. Biotechnol.*, **32**(9), 903–914.

Tenenhaus, M. (1998). *La régression PLS: théorie et pratique*. Editions Technip.

Tibshirani, R. (1996). Regression Shrinkage and Selection via the Lasso. *J. R. Stat. Soc. Ser. B. Stat. Methodol.*, **58**(1), 267–288.

Tsialikas, J. and Romer-Seibert, J. (2015). LIN28: roles and regulation in development and beyond. *Development*, **142**(14), 2397–2404.

Vargova, K., Curik, N., Burda, P., Basova, P., Kulvait, V., Pospisil, V., Savvulidi, F., Kokavec, J., Necas, E., Berkova, A., *et al.* (2011). Myb transcriptionally regulates the mir-155 host gene in chronic lymphocytic leukemia. *Blood*, **117**(14), 3816–3825.

Wells, C. A., Mosbergen, R., Korn, O., Choi, J., Seidenman, N., Matigian, N. A., Vitale, A. M., and Shepherd, J. (2013). Stemformatics: visualisation and sharing of stem cell gene expression. *Stem Cell Res.*, **10**(3), 387–395.

Whitcomb, B. W., Perkins, N. J., Albert, P. S., and Schisterman, E. F. (2010). Treatment of batch in the detection, calibration, and quantification of immunoassays in large-scale epidemiologic studies. *Epidemiology (Cambridge, Mass.)*, **21**(Suppl 4), S44.

Yamamoto-Ibusuki, M., Yamamoto, Y., Fujiwara, S., Sueta, A., Yamamoto, S., Hayashi, M., Tomiguchi, M., Takeshita, T., and Iwase, H. (2015). C6orf97-esr1 breast cancer susceptibility locus: influence on progression and survival in breast cancer patients. *Eur J Human Genet*, **23**(7), 949–956.

Yu, J., Vodyanik, M. A., Smuga-Otto, K., Antosiewicz-Bourget, J., Frane, J. L., Tian, S., Nie, J., Jonsdottir, G. A., Ruotti, V., Stewart, R., *et al.* (2007). Induced pluripotent stem cell lines derived from human somatic cells. *Science*, **318**(5858), 1917–1920.